Chemometrics and Intelligent Laboratory Systems 125 (2013) 121–131

Contents lists available at SciVerse ScienceDirect

Chemometrics and Intelligent Laboratory Systems

journal homepage: www.elsevier.com/locate/chemolab

Four-way multivariate calibration using ultra-fast high-performance liquid chromatography with fluorescence excitation–emission detection. Application to the direct analysis of chlorophylls *a* and *b* and pheophytins *a* and *b* in olive oils

Valeria A. Lozano [a], Arsenio Muñoz de la Peña [b,*], Isabel Durán-Merás [b], Anunciación Espinosa Mansilla [b], Graciela M. Escandar [a]

[a] Instituto de Química Rosario (CONICET-UNR), Facultad de Ciencias Bioquímicas y Farmacéuticas, Universidad Nacional de Rosario, Suipacha 531, 2000, Rosario, Argentina
[b] Department of Analytical Chemistry, Faculty of Sciences, University of Extremadura, 06006, Badajoz, Spain

ARTICLE INFO

Article history:
Received 29 January 2013
Received in revised form 2 April 2013
Accepted 5 April 2013
Available online 12 April 2013

Keywords:
Elution time–emission wavelength–excitation wavelength data
Third-order multivariate calibration
Chlorophylls
Pheophytins
Olive oils

ABSTRACT

A four-way multivariate calibration approach, based on the combination of ultra-fasthigh-performance liquid chromatographic data and four-way algorithms, is described for the first time. To achieve this goal, several emission wavelength–elution time matrices (ETMs) were recorded as a function of the excitation wavelength. Each sample was injected into the chromatograph eight times, in sequential mode, each time exciting at a different wavelength across the excitation spectra of the compounds of interest, and the emission spectra were recorded along the full chromatogram using a fast scanning fluorescence detector. The data were obtained in a very short time with an ultrafast chromatographic system operating in gradient mode. The three-wayETM data thus obtained for the calibration sample set and for each of the test samples were joined into a single four-way array, which was subsequently analyzed with parallel factor analysis (PARAFAC), unfolded partial least-squares with residual trilinearization (U-PLS/RTL) and multi-way partial least-squares with residual trilinearization (N-PLS/RTL) multivariate calibration algorithms. Best results were found when either U-PLS/RTL or N-PLS/RTL algorithms were used to perform the multivariate calibration. The method was applied to the direct determination of chlorophylls *a* and *b* and pheophytins *a* and *b* in olive oil samples, in the presence of other interfering fluorescent compounds, and without previous sample treatment.

1. Introduction

In order to perform the quantitative analysis of selected analytes of interest, in complex samples, a great effort has been recently directed to the use of excitation–emission fluorescence spectroscopy, in combination with different multivariate calibration modeling tools. These approaches are related to the ability of multi-way calibration models to exploit the partial selectivity in the different modes of the data set. Examples of the use of multivariate analysis using excitation–emission fluorescence matrix (EEFM) data, constituting three-way arrays when data for a group of samples are joined, were summarized in two recent reviews [1,2], both reporting up-to-date applications in the biomedical, environmental and food analysis fields.

High performance liquid chromatography (HPLC), when combined with spectroscopic techniques, such as UV–visible diode-array detection (DAD) or fast-scanning fluorescence detection (FSFD) is also able to yield spectral-elution time matrix data. The spectroscopic response is arranged as a data matrix, where each column corresponds to a wavelength and each row corresponds to a different elution time, and second-order multivariate calibration can be applied to the corresponding three-way arrays, when full selectivity in the chromatographic separation is not achieved, even in the presence of unexpected components. Additional benefits are decreasing cost and times of analysis. Two recent reports deal with the advantages and drawbacks associated with the combination of multivariate calibration and chromatography, and pertinent references on the successful processing of spectroscopic–chromatographic data can be found [3,4].

Surprisingly, very few literature works concern the processing of three-wayHPLC data with fluorescence detection. Early reports used either a videofluorimeter as detector [5], or more usually FSFD, in the latter case for the determination of polycyclic aromatic hydrocarbons (PAHs) [6–8] and naphthalenesulfonates and naphthalenedisulfonates [9], fluoroquinolones [10] and pteridines [11,12].

On going to one dimension further, four-way data have been usually processed by resorting to the well-knownPARAFAC algorithm [13]. The combination of trilinear least-squares with residual trilinearization (TLLS/RTL) has also been proposed as a new algorithm for four-way

* Corresponding author. Tel.: +34 924289378.
E-mail address: arsenio@unex.es (A. Muñoz de la Peña).

0169-7439/$ – see front matter © 2013 Elsevier B.V. All rights reserved.
http://dx.doi.org/10.1016/j.chemolab.2013.04.005

data processing, and has shown to be useful for the analysis of complex samples [14,15]. Alternative methodologies based on the use of latent variables do also exist for processing four-way data, such as N-PLS and the unfolded variant U-PLS, both of them lacking the second-order advantage. However, when U-PLS and N-PLS are coupled to the separate procedure known as RTL, they are also able to achieve the second-order advantage [15–18]. Other methodologies can also be applied to these data by first unfolding them into matrices and then applying MCR-ALS [19].

However, only in a few cases that four-way data have been recorded and used to construct quantitative calibration models and to develop analytical methodologies. This may be attributed to the fact that the experimental acquisition of these data arrays is still difficult to implement. Hence, although one can imagine a large number of possible forms of obtaining four-way data, those commonly used are the following: 1) with a single instrument, EEMs as a function of reaction time [20–28], and 2) with hyphenated instruments, bidimensional chromatography with time of flight mass spectrometry (TOFMS) or DAD, such as GC × GC–TOFMS or LC × LC–DAD, and LC–DAD as a function of reaction time (GC = gas chromatography) [29].

Four-way data would display the obvious advantage of providing richer analytical information, implying more stable methods towards interferences and matrix effects, and less prone to minor changes in reaction conditions. This should allow for an improvement in predictive ability.

The color of olive oil is principally related to its perceived quality, and therefore to its acceptability. The economic importance of the appearance of the oils is unquestionable. The color of virgin olive oil is due to the natural pigments chlorophylls (chl), pheophytins (phe) and carotenoids [30]. The pigment content depends on widely changing variables such as the degree of fruit ripeness (green olives give a green oil because of the high chlorophyll and pheophytin content, and ripe olives give a yellow oil due to carotenoid pigments), environmental conditions, production zone, processing techniques [31] and storage conditions [32]. In addition, the chromatic intensities and pigment contents have been related with different extraction methodologies. In this sense, the contents of chlorophylls and derivatives have been used to identify if the olive oils have been subject to deodorization, a fraudulent treatment [33].

Determination of chlorophylls and pheophytins in olive oils usually involves HPLC methods with UV detection. These compounds display a hydrophobic nature, due to the long hydrocarbon side chain (phytol chain) attached to the chlorin ring. This fact makes the analysis difficult by reversed-phaseHPLC (RP-HPLC): in general, the analysis time is long and the use of an ion-pair reagent in the mobile phase is needed. In all proposed methods, it is necessary to isolate the pigment fraction of olive oils by liquid–liquid extraction or by solid-phase extraction [34]. The analysis of the pigment fraction has been usually performed by reversed-phaseion-pair chromatography with UV–vis detection [35,36] or in series with a fluorescence detector [37].

The bibliography about the application of multivariate methods to the quantification of these pigments in olive oils is scarce [38–40]. In a previous paper, the resolution of the mixtures of chl *a* and *b* and phe *a* and *b* has been accomplished by PLS regression of the excitation spectra [41].

In this report, we describe, for the first time, a four-way multivariate calibration approach based on data obtained using UHPLC (ultra-fast HPLC) in combination with a fast-scanning spectrofluorometer as detector, that allows the recording of a complete emission scan in a short run time and thus, emission–elution time three-way matrices (ETMs) have been easily measured for each experimental sample. The third mode is obtained by recording each ETM at different excitation wavelengths. These four-way data, based on elution time–fluorescence excitation–emission measurements, were processed with several multi-way algorithms such as PARAFAC,U-PLS and N-PLS, with the latter two conveniently combined with RTL. This procedure has been applied to the four-way data corresponding to mixtures of chlorophylls and pheophytins in olive oil samples, without pretreatment of the samples, and without the isolation of the pigment fraction. The best results were obtained with the U-PLS/RTL and N-PLS/RTL combinations. The developed method enabled us to determine the pigments, some of them with overlapping profiles, in olive oils, in a short analysis time and in the presence of other interfering fluorescent compounds.

2. Materials and methods

2.1. Reagents and solutions

Chlorophylls *a* and *b* (chl *a* and chl *b*) were obtained from Sigma-Aldrich Chemical Co. and used as received. Stock solutions of chlorophylls *a* and *b* were prepared by dissolving the contents of ampules containing 1 mg of each chlorophyll, in 25.00 mL of acetone and stored at −4 °C in darkness. The acetone was purchased from Merck (Darmstadt, Germany). Pheophytin (phe) stock solutions of 40 μg mL^{-1} were prepared according to a previously described procedure [41]. Solutions of the four pigments of lower concentrations were prepared by appropriate dilution with acetone. These solutions were stored at −4 °C. All other chemicals utilized were of analytical reagent grade or better.

Methanol and 1-propanol, HPLC-grade, were purchased from Sigma (Spain). Ultrapure water provided by a Milli-Q purification system was used. Solvents and samples used to perform the chromatographic technique were filtered through 0.22 μm nylon filter membranes before each injection.

2.2. Apparatus and software

HPLC was carried out on an Agilent 1260 Infinity Series equipped with a degasser, a quaternary pump, a column oven, a manual six-way injection valve with a 10 μL fixed loop, a multi-scan fluorescent detector (G1321B FLD) and the ChemStation software package to control the instrument and data acquisition. The analytical column used was a Poroshell 120 EC-C18 column (4.6 × 50 mm, 2.7 μm, Agilent Technologies, Inc.). The Poroshell 120 packing has a solid core of 1.7 μm in size with a porous outer layer 0.5 μm thick and a total particle size of 2.7 μm. The column temperature was set at 20 °C. Data acquisition and instrument control were performed on the HPLC 1260 software package. The mobile phase consisted of a mixture of methanol and 1-propanol and these components were filtered through a 0.22 μm membrane nylon filter and degassed by ultrasonication before use. The flow rate was 2.0 mL min^{-1}. The elution was made by applying a gradient mode increasing the percentage of 1-propanol. The gradient program was the following: from 0 to 0.2 min the percentage of 1-propanol was 40%; from 0.2 to 0.3 min the percentage of 1-propanol was increased from 40 to 70% and then was maintained constant until 0.9 min; from 0.9 to 1.0 min the percentage of 1-propanol was decreased up to 40% and from 1 to 1.1 min, was maintained constant at 40%. Sequential mode was used and, for each sample, eight chromatograms were obtained exciting at eight different excitation wavelengths (from 350 to 490 nm in 20 nm steps) and recording the emission spectra from 620 nm to 680 nm every 1 nm, in 1.7 s time steps (the data points between 0 and 0.27 min were discarded because of a dead-time artifact). Each run was accomplished in 1.1 min and the complete analysis for a specific sample was carried out in 8.8 min. These matrices were then saved in ASCII format, and transferred to a PC based on an AMD Athlon dual core microprocessor for subsequent manipulation.

All calculations were done using MATLAB 7.0 [42], using different routines and graphical interfaces: MVC3 (MultiVariate Calibration for third-order), an integrated MATLAB toolbox for third-order calibration developed by Olivieri et al. [43], which allows performing third-order calibration with different modeling methods, including PARAFAC[13], U-PLS and N-PLS, both coupled to RTL[15,18]. The software can be freely

downloaded from the webpage www.iquir-conicet.gov.ar/descargas/mvc3.rar.

2.3. Calibration and validation samples

The experimental procedure corresponding to the four-way analysis for chl *a*, chl *b*, phe *a* and phe *b* was developed preparing a calibration set of 25 samples: 16 of these samples corresponding to the concentrations provided by a full factorial design with two levels for each analyte, 2 replicates of the central point, 6 samples containing one or two of the studied analytes at the average calibration concentration, and a final blank sample only containing methanol:1-propanol 60:40 (v/v). The tested concentrations were in the range of 0.5–1.5 μg mL^{-1} for each analyte. A validation set of 7 samples was prepared, employing different concentrations than those used for calibration and following a random design, i.e., choosing the validation concentrations by generating random numbers, equally distributed within the analyte calibration ranges. The specific calibration and validation concentrations are provided in Tables 1 and 2, respectively, and the ranges were established on the analysis of the linear fluorescence-concentration range for each analyte. Calibration and validation samples were prepared by measuring appropriate aliquots of standard solutions, placing them in 5.00 mL volumetric flasks in order to obtain the desired concentrations, and completing to the mark with the mobile phase. Injection into the chromatographic system was made in random order and in different days.

2.4. Olive oil samples

The olive oil samples (approximately 1 g) with and without addition of different amounts of each pigment were diluted to 10 mL with 1-propanol. Aliquots of 1 mL of these solutions were diluted with 3.0 mL of 1-propanol and with 6.0 mL of methanol up to a final volume of 10.0 mL. After that, aliquots (10 μL) of each sample were injected in the chromatographic system to obtain the chromatograms at the different selected excitation wavelengths. The four-way arrays obtained were used to measure the pigments in the olive oil samples.

Table 1
Calibration and validation concentrations (μg mL^{-1}) employed for quantitation of the chl *a*, chl *b*, phe *a* and phe *b*.

Sample	Chl *a*	Chl *b*	Phe *a*	Phe *b*
1	0.5	0.5	0.5	0.5
2	1.5	0.5	0.5	0.5
3	0.5	1.5	0.5	0.5
4	1.5	1.5	0.5	0.5
5	0.5	0.5	1.5	0.5
6	1.5	0.5	1.5	0.5
7	0.5	1.5	1.5	0.5
8	1.5	1.5	1.5	0.5
9	0.5	0.5	0.5	1.5
10	1.5	0.5	0.5	1.5
11	0.5	1.5	0.5	1.5
12	1.5	1.5	0.5	1.5
13	0.5	0.5	1.5	1.5
14	1.5	0.5	1.5	1.5
15	0.5	1.5	1.5	1.5
16	1.5	1.5	1.5	1.5
17	1.0	1.0	1.0	1.0
18	1.0	1.0	1.0	1.0
19	1.0	0.0	0.0	0.0
20	0.0	1.0	0.0	0.0
21	0.0	0.0	1.0	0.0
22	0.0	0.0	0.0	1.0
23	1.0	0.0	1.0	0.0
24	0.0	1.0	0.0	1.0
25	0.0	0.0	0.0	0.0

Table 2
Predicted concentrations (μg mL^{-1}) in validation samples using PARAFAC,U-PLS and N-PLS.

								RMSEP[a]	REP[b]
	Chl *a*								
Actual	0.40	0.80	1.20	1.40	0.60	0.90	1.00		
PARAFAC	0.30	0.35	0.98	1.44	0.30	0.49	0.72	0.29	29
U-PLS	0.43	0.85	1.14	1.31	0.56	0.89	1.00	0.05	5
N-PLS	0.40	0.85	1.13	1.32	0.56	0.90	1.00	0.05	5
	Chl *b*								
Actual	1.40	0.40	0.80	1.20	0.90	0.60	1.00		
PARAFAC	1.40	0.21	0.21	1.47	0.30	0.21	0.79	0.38	38
U-PLS	1.31	0.44	0.86	1.04	0.89	0.48	1.00	0.09	9
N-PLS	1.48	0.34	0.73	0.88	0.81	0.44	0.97	0.15	15
	Phe *a*								
Actual	1.20	1.40	0.40	0.80	0.60	0.90	1.00		
PARAFAC	1.21	1.38	0.31	0.31	0.31	0.36	0.78	0.31	31
U-PLS	1.22	1.34	0.37	0.74	0.54	0.86	1.04	0.05	5
N-PLS	1.29	1.34	0.35	0.74	0.53	0.85	1.02	0.06	6
	Phe *b*								
Actual	0.80	1.20	1.40	0.40	0.90	0.60	1.00		
PARAFAC	0.38	1.26	1.26	0.30	0.33	0.30	0.72	0.32	32
U-PLS	0.84	1.27	1.24	0.34	0.81	0.57	0.99	0.08	8
N-PLS	0.83	1.28	1.28	0.37	0.82	0.58	1.00	0.06	6

[a] RMSEP, root mean square error prediction in μg mL^{-1}.
[b] REP, relative error prediction in %.

3. Theory

3.1. PARAFAC

After measuring third-order data for a set of samples, each of them as a $J \times K \times L$ array (J, K and L are the number of data points in each of the three modes), the I training arrays $\underline{\mathbf{X}}_{i,\mathrm{cal}}$ are joined with the unknown sample array $\underline{\mathbf{X}}_{\mathrm{u}}$ into a four-way data array $\mathbf{X}$, whose dimensions are $[(I+1)\times J\times K\times L]$. Provided $\mathbf{X}$ follows a quadrilinear PARAFAC model, it can be written in terms of four vectors for each responsive component, designated as $\mathbf{a}_n$, $\mathbf{b}_n$, $\mathbf{c}_n$ and $\mathbf{d}_n$, and collecting the relative concentrations $[(I+1)\times 1]$ for component n, and the profiles in the three modes ($J\times 1$), ($K\times 1$) and ($L\times 1$), respectively. The specific expression for a given element of $\mathbf{X}$ is [44]

$$X_{ijkl} = \sum_{n=1}^{N} a_{in} b_{jn} c_{kn} d_{ln} + E_{ijkl} \quad (1)$$

where N is the total number of responsive components, a_{in} is the relative concentration of component n in the ith sample, and b_{jn}, c_{kn} and d_{ln} are the fluorescence intensities at the emission wavelength j, excitation wavelength k and elution time l, respectively. The values of E_{ijkl} are the elements of the array $\mathbf{E}$, which is a residual error term of the same dimensions as $\mathbf{X}$. The column vectors $\mathbf{a}_n$, $\mathbf{b}_n$, $\mathbf{c}_n$ and $\mathbf{d}_n$ are collected into the corresponding loading matrices $\mathbf{A}$, $\mathbf{B}$, $\mathbf{C}$ and $\mathbf{D}$ ($\mathbf{b}_n$, $\mathbf{c}_n$ and $\mathbf{d}_n$ are usually normalized to unit length).

The model described by Eq. (1) defines a decomposition of $\mathbf{X}$ which provides access to emission ($\mathbf{B}$) and excitation spectral profiles ($\mathbf{C}$), elution time profiles ($\mathbf{D}$) and relative concentrations ($\mathbf{A}$) of individual components in the $(I+1)$ mixtures, whether they are chemically known or not. This constitutes the basis of the second-order advantage. The decomposition is usually accomplished through an alternating least-squares minimization scheme [45,46].

Initializing PARAFAC for the study of four-way arrays can be done using singular value decomposition vectors, spectral and chromatographic data which are known in advance for pure components, or by the loadings giving the best fit after small PARAFAC runs involving both singular value decomposition vectors and several sets of orthogonal random loadings. These options are implemented in the PARAFAC package [47].

The number of responsive components (N) can be estimated by several methods. A useful technique is CORCONDIA, a diagnostic tool considering the PARAFAC internal parameter known as core consistency [48,49]. Another useful technique is the consideration of the PARAFAC residual error, i.e., the standard deviation of the elements of the array **E** in Eq. (1)[45]. Usually this parameter decreases with increasing N, until it stabilizes at a value compatible with the instrumental noise (the latter can be assessed by blank replicate measurements). A reasonable choice for N is thus the smallest number of components for which the residual error is not statistically different than the instrumental noise.

Identification of the chemical constituents under investigation is done with the aid of the three estimated profiles: emission spectrum, excitation spectrum and chromatographic profile, and comparing them with those for a standard solution of the analyte of interest. This is required since the components obtained by decomposition of **X** are sorted according to their contribution to the overall spectral variance, and this order is not necessarily maintained when the unknown sample is changed.

Absolute analyte concentrations are obtained after calibration, because the four-way array decomposition only provides relative values (**A**). Calibration is done by means of the set of standards with known analyte concentrations (contained in an $I \times 1$ vector **y**), and regression of the first I elements of column $\mathbf{a}_n$ against **y**:

$$k = \mathbf{y}^{+} \times [a_{In}|\ldots|a_{In}] \tag{2}$$

where "+" implies taking the pseudo-inverse. Conversion of relative to absolute concentration of n in the unknown proceeds by division of the last element of column $\mathbf{a}_n$ [$a_{(I+1)n}$] by the slope of the calibration graph k:

$$y_u = a_{(I+1)n}/k. \tag{3}$$

The above procedure is repeated for each new test sample analyzed.

3.2. U-PLS/RTL

For four-way calibration, U-PLS/RTL constitutes an extension of U-PLS/RBL one further mode [15], and will be briefly described in this section. When using four-way data, in the U-PLS method, the original matrix data is transformed into uni-dimensional arrays (vectors) by concatenating (unfolding) the original three-dimensional information, and concentration information is first employed into the calibration step (without including data for the unknown sample) [50]. The calibration third-order arrays are vectorized (unfolded) and a usual U-PLS model is calibrated with these data and the vector of calibration concentrations **y** ($I \times 1$). This provides a set of loadings **P** and weight loadings **W** (both of size $JKL \times A$, where A is the number of latent factors), as well as regression coefficients **v** (size $A \times 1$). The parameter A can be selected by techniques such as leave-one-outcross-validation[51]. If no unsuspected interferences occur in the test sample, **v** can be employed to estimate the analyte concentration:

$$y_u = \mathbf{t}_u{}^{T}\mathbf{v} \tag{4}$$

where $\mathbf{t}_u$ (size $A \times 1$) is the test sample score, obtained by a projection of the (unfolded) data for the test sample $\underline{\mathbf{X}}_u$ [vec($\underline{\mathbf{X}}_u$), size ($JKL \times 1$)] onto the space of the A latent factors:

$$\mathbf{t}_u = \left(\mathbf{W}^{T}\mathbf{P}\right)^{-1}\mathbf{W}^{T}\mathbf{vec}\left(\underline{\mathbf{X}}_u\right). \tag{5}$$

When uncalibrated constituents occur in $\underline{\mathbf{X}}_u$, the sample scores given by Eq. (5) are not suitable for analyte prediction using Eq. (4). In this case, the residuals of the U-PLS prediction step will be abnormally large in comparison with the typical instrumental noise assessed by replicate measurements:

$$s_p = \left|\left|\mathrm{vec}\left(\mathbf{E}_p\right)\right|\right|/(JKL-A)^{1/2} = ||\mathrm{vec}\left(\underline{\mathbf{X}}_u\right) - \mathbf{P}\left(\mathbf{W}^{T}\mathbf{P}\right)^{-1}\mathbf{W}^{T}\mathrm{vec}\left(\underline{\mathbf{X}}_u\right)||/(JKL-A)^{1/2} = \\ = ||\mathrm{vec}\left(\underline{\mathbf{X}}_u\right) - \mathbf{P}\,\mathbf{t}_u||/(JKL-A)^{1/2} \tag{6}$$

where $||\cdot||$ indicates the Euclidean norm, and $JKL - A$ corresponds to the degree of freedom (number of variables minus number of adjustable parameters).

If interferent components occur in the test sample, the situation can be handled by RTL, based on a Tucker3 decomposition that models the interferent effects, as already described [15]. RTL aims at minimizing the norm of the residual vector $\mathbf{e}_u$, computed while fitting the sample data to the sum of the relevant contributions to the sample signal. For a single interferent the relevant expression is:

$$\mathrm{vec}\left(\underline{\mathbf{X}}_u\right) = \mathbf{P}\,\mathbf{t}_u + g_{int}(\mathbf{d}_{int}\otimes\mathbf{c}_{int}\otimes\mathbf{b}_{int}) + \mathbf{e}_u \tag{7}$$

where $\mathbf{b}_{int}$, $\mathbf{c}_{int}$ and $\mathbf{d}_{int}$ are normalized profiles in the three modes for the interference and g_{int} is the first core element obtained for Tucker3 analysis of $\underline{\mathbf{E}}_p$ in the following way:

$$(g_{int}, \mathbf{b}_{int}, \mathbf{c}_{int}, \mathbf{d}_{int}) = \mathrm{Tucker3}\left(\underline{E}_p\right). \tag{8}$$

During this RTL procedure, **P** is kept constant at the calibration values and $\mathbf{t}_u$ is varied until $||\,\mathbf{e}_u\,||$ is minimized. The minimization can been carried out using either a Gauss–Newton (GN) procedure or an alternating least squares algorithm, in both cases starting with $\mathbf{t}_u$ from Eq. (5). Once $||\,\mathbf{e}_u\,||$ is minimized in Eq. (7), the analyte concentrations are provided by Eq. (4), by introducing the final $\mathbf{t}_u$ vector found by the RTL procedure.

The number of interferents N_i can be assessed by comparing the final residuals s_u with the instrumental noise level:

$$s_u = ||\mathbf{e}_u||/[JKL-(N_c + N_i)]^{1/2} \tag{9}$$

where $\mathbf{e}_u$ is from Eq. (7) and N_c is the number of calibrated analytes. Typically, a plot of s_u computed for trial number of components will show decreasing values, starting at s_p when the number of components is equal to A (the number of latent variables used to described the calibration data), until it stabilizes at a value compatible with the experimental noise, allowing to locate the correct number of components.

To analyze the presently discussed data, the Tucker3 model in Eq. (8) is constructed by restricting the loadings to be orthogonal, and with no special constraints on the core elements. For a single unexpected component, this analysis is straightforward, and provides the corresponding interferent profiles in the three modes. For additional unexpected constituents, however, the retrieved profiles no longer resemble true spectra (or elution time profiles). Moreover, in this latter case, several different Tucker3 models could in principle be constructed, because the number of loadings may be different in each mode. We notice that the aim which guides the RTL procedure is the minimization of the residual error term s_u of Eq. (9) to a level compatible with the degree of noise present in the measured signals. Therefore, if two unexpected components are considered, for example, one should explore the possible Tucker3 models having one or two loadings in each mode, and select the simplest model giving a residual value of s_u which is not statistically different than the minimum one. For more unexpected components a similar procedure is recommended. The final Tucker3 model selected to model the unexpected effects is the simplest one which provides a value of s_u which is not statistically different than the noise level.

We note that two different residual parameters appear in the above discussion, which should not be confused: s_p [Eq. (6)] corresponds to the difference between the test sample signal and that model by U-PLS before the RTL procedure, while s_u [Eq. (9)] arises from the difference after the RTL modeling of the interferent effects. Hence it is the latter one which should be comparable to the instrumental noise level if RTL is successful.

3.3. N-PLS/RTL

In the N-PLS method applied to third-order data, concentration information is employed in the calibration step, without including data for the unknown sample. The I calibration data arrays, together with the vector of calibration concentrations $\mathbf{y}$ (size $I \times 1$) are employed to obtain sets of loadings $\mathbf{W}^j$, $\mathbf{W}^k$ and $\mathbf{W}^l$ (of sizes $J \times A$, $K \times A$ and $L \times A$, where A is the number of latent factors), as well as regression coefficients $\mathbf{b}$ (size $A \times 1$) [48]. The parameter A can be selected by techniques such as leave-one-outcross-validation[51]. If no unexpected components occurred in the test sample, $\mathbf{b}$ could be employed to estimate the analyte concentration according to:

$$y_u = \mathbf{t}_u{}^T\mathbf{b} \tag{10}$$

where $\mathbf{t}_u$ is the test sample score vector, obtained by appropriate projection of the test data onto the calibration loading matrices. When unexpected constituents occur in the unknown sample, the latter scores are unsuitable for analyte prediction through Eq. (10). In this case, it is useful to consider the residuals of the N-PLS modeling of the test sample signal [s_p, see Eq. (11) below] before prediction is made. These residuals will be abnormally large in comparison with the typical instrumental noise level:

$$s_p = \left\|\mathbf{e}_p\right\|/(JKL\text{–}A)^{1/2} = \left\|\mathrm{vec}(X_u)\text{–}\mathrm{vec}\left(\hat{X}_u\right)\right\|/(JKL\text{–}A)^{1/2} \tag{11}$$

where $\hat{X}_u$ is the sample three-way data array ($\mathbf{X}_u$) reconstructed by the N-PLS model and $\|\cdot\|$ indicates the Euclidean norm.

This situation can be handled by a separate procedure called residual trilinearization, based on the Tucker3 model of the unexpected effects, as discussed above for U-PLS/RTL. In the case of N-PLS/RTL, the analogous expression to Eq. (7) is:

$$X_u = \mathrm{reshape}\left\{\mathbf{t}_u\left[\left(\mathbf{W}^j|\otimes|\mathbf{W}^k\right)|\otimes|\mathbf{W}^1\right]\right\} + \mathrm{Tucker3}\left(\hat{X}_u\text{–}X_u\right) + E_u \tag{12}$$

where 'reshape' indicates transforming a $JKL \times 1$ vector into a $J \times K \times L$ three-way array, and $|\otimes|$ indicates the Kathri–Rao operator [48]. During this RTL procedure, the weight loadings $\mathbf{W}^j$, $\mathbf{W}^k$ and $\mathbf{W}^l$ are kept constant at the calibration values, and $\mathbf{t}_u$ is varied until the final RTL residual error s_u is minimized using a Gauss–Newton procedure, with s_u given by:

$$s_u = ||E_u||/\left[(JKL\text{–}(N_c + N_i)\right]^{1/2} \tag{13}$$

where $\mathbf{E}_u$ is from Eq. (12). Once this is done, the analyte concentrations are provided by Eq. (10), by introducing the final $\mathbf{t}_u$ vector found by the RTL procedure. The considerations discussed above concerning the Tucker3 model of Eq. (12) do also apply to N-PLS/RTL.

4. Experimental

4.1. Fluorescence properties of analytes

The native fluorescence of these compounds is well-known and there are many reports about the fluorescence of chl *a* in different solvents [52]. However, as regards the fluorescence of the other derivatives, such as chl *b* and pheophytins, data are scarce. In a first phase, we studied the analyte fluorescence in the solvents to be used as mobile phase, e.g., methanol:1-propanol 60:40 (v/v). Fig. 1 shows the excitation and emission spectra for 1.00 μg mL^{-1} of the studied analytes in this solvent mixture. They were recorded in wide spectral excitation and emission ranges: 300–500 nm and 600–720 nm, respectively. The profiles of emission spectra are very similar for the four components, and their maxima are very close, being 672 nm for chl *a*, 663 nm for chl *b*, 671 nm for phe *a*, and 658 nm for phe *b*. The largest differences correspond to the excitation spectra. No substantial differences were detected in the position of excitation and emission maxima with respect to other solvents [52]. The quantum yield of chlorophylls and pheophytins in different solvents has been previously described. For chlorophyll *a*, quantum yield values of 0.30 and 0.23, in acetone and in methanol, respectively, have been reported. For chlorophyll *b* the values are 0.09 and 0.10, respectively, and for pheophytin *a* in benzene, the reported quantum yield is 0.117 [53]. In our experimental conditions, when the mobile phase is methanol:1-propanol, 30:70 (v:v), the fluorescence of the chlorophylls and of the pheophytins is about 60% lower than in the pure solvents.

Although the fluorescence quantum yields in the selected mixture of solvents are smaller than those found in acetone or in methanol, this mobile phase mixture allows the direct analyses of the pigments in olive oil without the need of a previous extraction step.

4.2. Optimization of the chromatographic conditions

Usually, the HPLC procedures for the determination of green pigments in olive oils involve the previous extraction of the pigment fraction by either liquid–liquid or solid-phase extractions. These procedures are very laborious, and the recoveries are not satisfactory for all pigments, due to their different polarities [30]. Currently, the LC proposed methods use UV detection; fluorescence detection is less used [37]. Also, one of the components of the mobile phase is usually an ion-pair reagent [30,34]. This limits the proportion of the organic modifier in the mobile phase, because high quantities can cause the precipitation of the ion-pair reagent. Finally, the experimental time for a single run in most methods is ca. 30 min.

An objective of the present study was to decrease the analysis time. To achieve this goal, a short column with 2.7 μm particle size was used, as these columns have similar efficiency to sub-2 μm columns and, allow working with 40–50% less pressure. The first step consisted in optimizing the composition of the mobile phase and

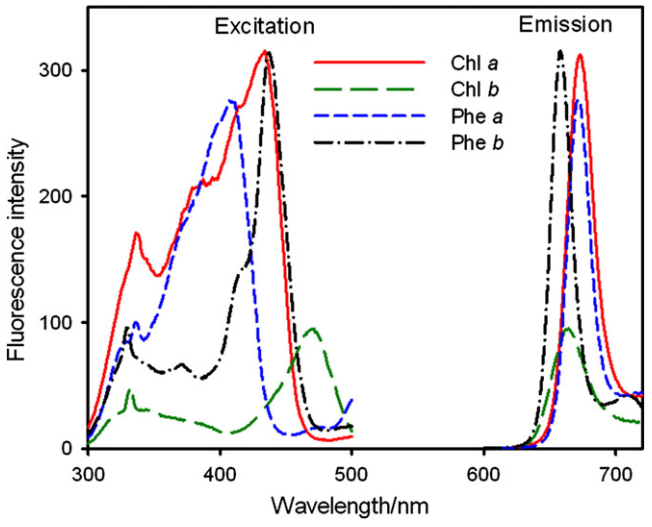

Fig. 1. Excitation and emission spectra of chl *a*, chl *b*, phe *a* and phe *b* in methanol-1–propanol (60:40, v/v). All concentrations were 1.00 μg mL^{-1}.

flow rate, with the aim of keeping the separation time as short as possible.

The composition of the mobile phase was studied with the purpose of directly analyzing the olive oil samples, hence the first challenge was to select solvent mixtures that were miscible with the oils. Different solvent mixtures were tested, namely methanol–acetone, methanol-1–propanol, and acetonitrile–1-propanol. The best results were obtained with a mixture of methanol and 1-propanol (60:40, v/v). The flow rate was varied between 1.2 and 2 mL min^{-1}, and the latter value was chosen because the analysis time was smaller, i.e., on the order of 1 min, as desired. A gradient elution was necessary because of the wide range in capacity factors of the analytes in study. The initial percentage of 1-propanol (40%) was varied in order to optimize the resolution between the two chlorophylls. However, under these conditions, the elution of the pheophytins, which are less polar than chlorophylls, required a run time of ca. 3 min. Then, different elution gradients using increasing percentages of 1-propanol were tested, in order to achieve the elution of the four analytes in about 1 min. Finally, the gradient that provides the best relation between run time and resolution was as follows: methanol:1-propanol, 60:40 (v/v) during 0.2 min, followed by a linear gradient to 70% of 1-propanol and then constant until 0.9 min, from 0.9 to 1.0 min the percentage of 1-propanol decreased linearity to 40% and finally, this proportion was maintained constant up to 1.1 min. Different injection volumes of 5, 10 and 20 μL were also tested, choosing a 10 μL loop as optimum.

Fig. 2 shows the profile of the optimized elution gradient, and a chromatogram of standard solutions containing 1.0 μg mL^{-1} of each analyte, eluted under the optimized conditions. The complete elution time was 1.1 min.

In these conditions, univariate calibration curves (peak areas vs. analyte concentration) were constructed for the quantification of chl *a*, chl *b*, phe *a* and phe *b*, in order to check the linear analytical range for the isolated analytes. Solutions for calibration curves were prepared by convenient dilution of the standard solutions with mobile phase (methanol:1-propanol, 60:40, v/v), in order to obtain concentrations in the range of 0.5–1.5 μg mL^{-1} for each analyte. The data were fitted by standard least-squares regression and the square of the correlation coefficient (R^2) obtained were 0.9935 for chl *a*, 0.9967 for chl *b*, 0.9881 for phe *a* and 0.9995 for phe *b*.

As can be seen in Fig. 2, these analytes cannot be accurately quantitated by univariate calibration, because the resolution between all peaks is lower than the acceptable minimum. The resolution was first attempted using second-order calibration based on emission–elution time data, obtained by exciting all analytes at a compromise fixed wavelength. In this case, an extensive overlapping occurs in both elution and emission modes, and the sensitivity for phe *a* and chl *b* is not adequate. Thus, in complex cases such as the present one, it is necessary to employ advanced multi-way modeling techniques for quantifying the four pigments. Third-order multivariate calibration is known to provide increased sensitivity and selectivity but, up to now, these algorithms have been used mainly with excitation–emission matrices, and no data has been reported about its application to four-way data obtained with HPLC.

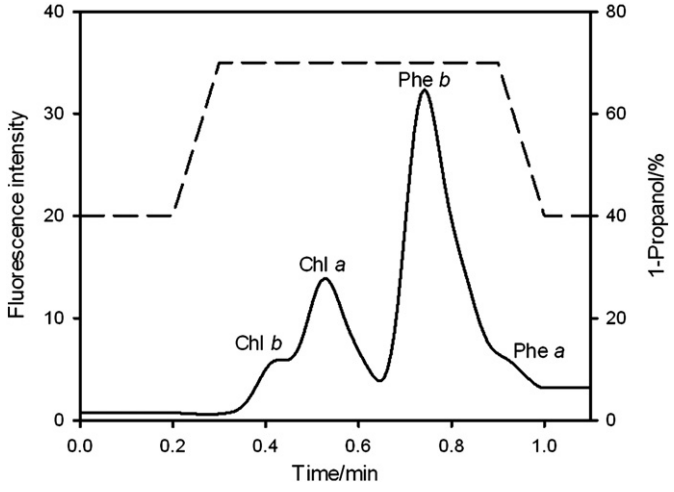

Fig. 2. Liquid chromatogram of chl *a*, chl *b*, phe *a* and phe *b* for a typical validation sample, containing 1.00 μg mL^{-1} of each compound (solid line). LU: luminescence units. Mobile phase: gradient program as a function of 1-propanol (%) during the analysis time (dashed line).

4.3. Four-way data recording

Fig. 3 shows the three-way data array structure obtained in this work, following the excitation wavelengths of the matrices for one of the calibration mixtures (1.00 μg mL^{-1} of each analyte) in the selected spectral ranges. For each sample, 61 emission spectra have been recorded between 620 and 680 nm, with data interval of 1 nm, and at intervals of 1.8 s. The excitation wavelengths were ranged between 350 and 490 nm in steps of 20 nm. It can be appreciated that the emission intensity of the analytes varies considerably as a function of the excitation wavelengths. These eight matrices were then mathematically assembled using MATLAB commands to obtain a three-way array for each sample. In Fig. 4 the three-way array, obtained by concatenating the eight emission–elution time matrices at the different excitation wavelengths, is reported. This data ensemble corresponds to a single calibration sample.

Fig. 5 shows the excitation–emission matrices for different elution times, extracted from the three-way array. It shows a contour plot of the complete landscape of fluorescence intensity as a function of excitation and emission wavelengths at ten different elution times, for the same sample used in Fig. 3. It can be appreciated that the fluorescence intensity of each of the analytes increases at different elution times, and highlights the fact that a significant overlapping occurs between chlorophylls and pheoppytins. At 0.36 min the first peak corresponding to chl *b* begins to elute, finishing at 0.45 min, and chl *a* starts appearing reaching its maximum at 0.54 min. Phe *b* appears at 0.72 min and continues until 0.81 min, and phe *a* comes out at 0.90 min.

4.4. Validation samples

The set of 7 validation samples (Table 2) was investigated with the aid of PARAFAC,U-PLS and N-PLS, employing the MVC3 interface. The first step is the assessment of the correct number of sample constituents or the latent variables. For PARAFAC, the number of components was selected applying the so-called core consistency analysis (CORCONDIA) [49,50], and for U-PLS and N-PLS, a leave-one-sample-out cross-validation procedure, according to the criterion of Haaland and Thomas [51], was performed. In these last two algorithms, the optimum number of factors was estimated by calculating the ratios $F(A) = \mathrm{PRESS}(A < A^*) / \mathrm{PRESS}(A)$ [where $\mathrm{PRESS} = \Sigma(y_{i,act} - y_{i,pred})^2$, A is a trial number of factors and A^* corresponds to the minimum PRESS] and selecting the number of factors leading to a probability of less than 75% that $F > 1$. For the three calibration models, the estimated number of components was 4 in all validation samples, which can be justified taking into account the presence of the four analytes.

The nominal and predicted concentration results corresponding to the application of PARAFAC,U-PLS and N-PLS, and the statistical parameters (root mean square errors and relative errors of predictions) obtained in the analysis of validation samples, are collected in Table 2. It is noticeable that the results obtained with PARAFAC are not good, probably due to the fact that PARAFAC requires that the data show the property of quadri-linearity, which can be lost if chromatographic elution times are not exactly reproducible and if one (or both) of the spectral modes show a great overlapping, as occurs in this case with the

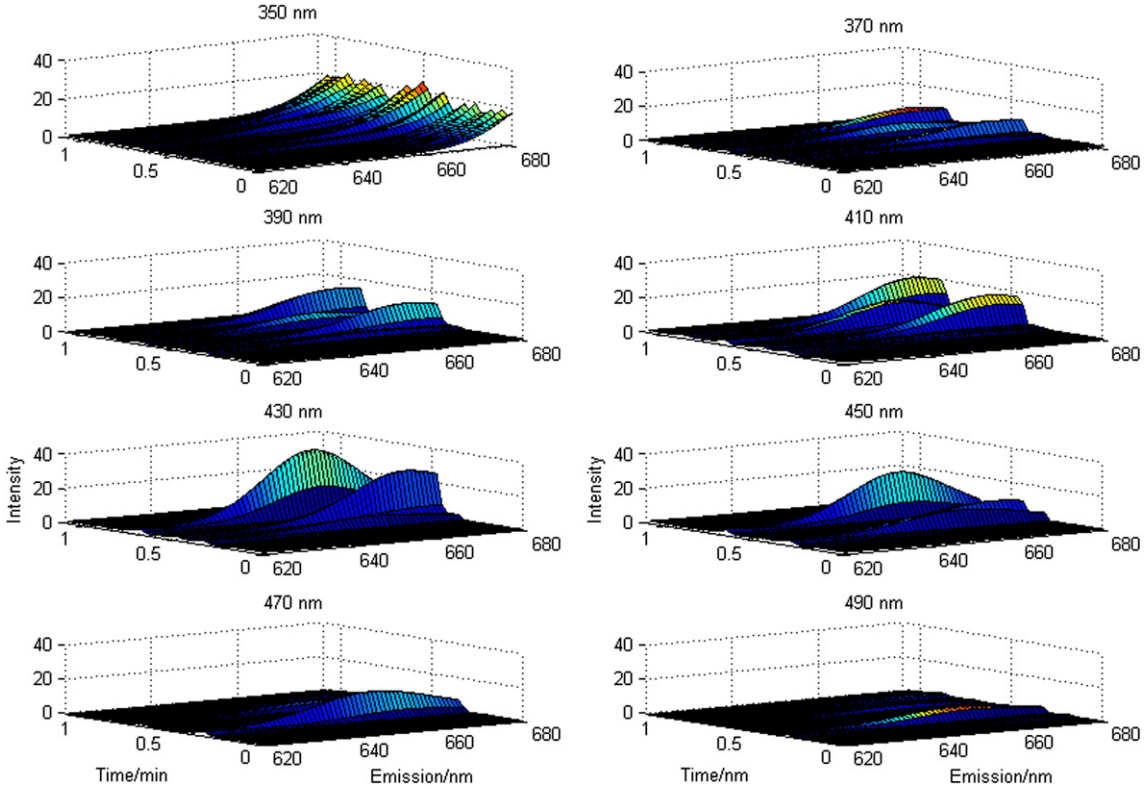

Fig. 3. Data matrices obtained for a typical validation sample as a function of emission wavelength and retention time, varying the excitation wavelengths from 350 nm to 490 nm in steps of 20 nm.

emission spectra of the four analytes. However, the results obtained with U-PLS or N-PLS are very satisfactory. The N-PLS results are similar to those obtained with its unfolded counterpart, U-PLS, and better than those from PARAFAC. The better predictive ability of U-PLS and N-PLS may be due to two reasons: (1) in principle, these algorithms do not require quadri-linearity, and (2) both have a more flexible internal structure. This may be an indication that this latent structure method may be better prepared to cope with the problems of severe spectral

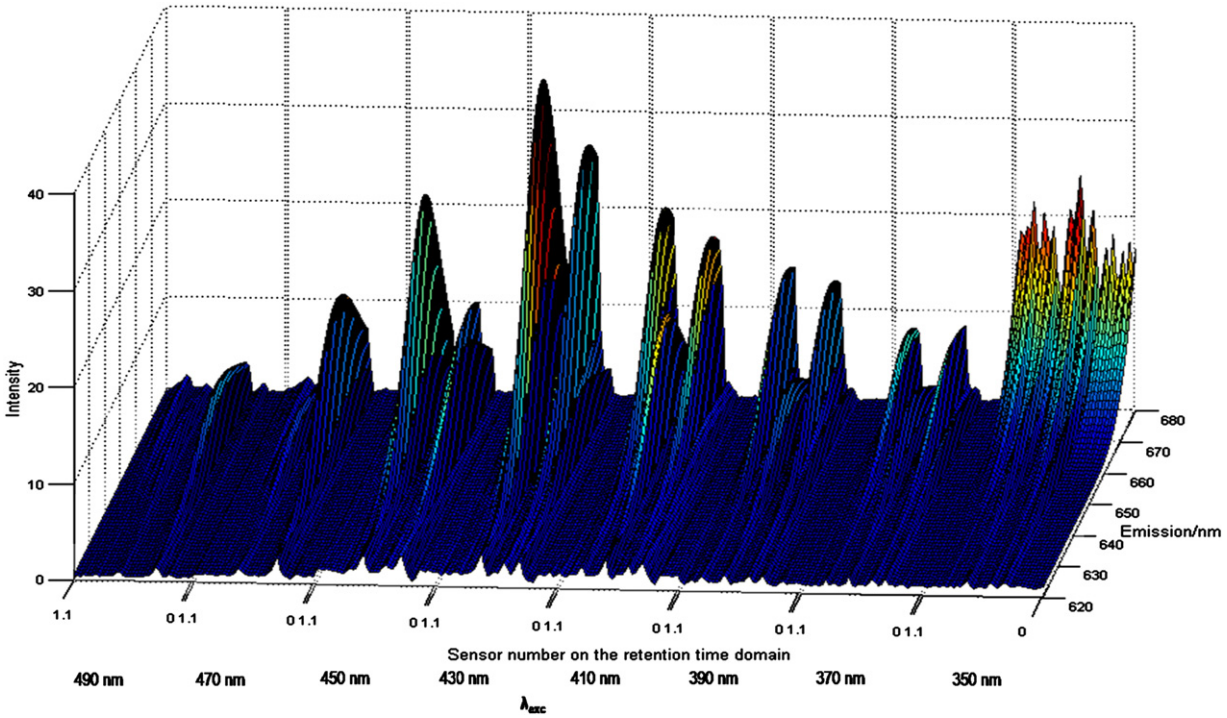

Fig. 4. Four-way array obtained by concatenating each of the three-way data (excitation wavelengths were from 350 to 490 nm in steps of 20 nm). Each chromatographic run is performed between 0 and 1.1 min.

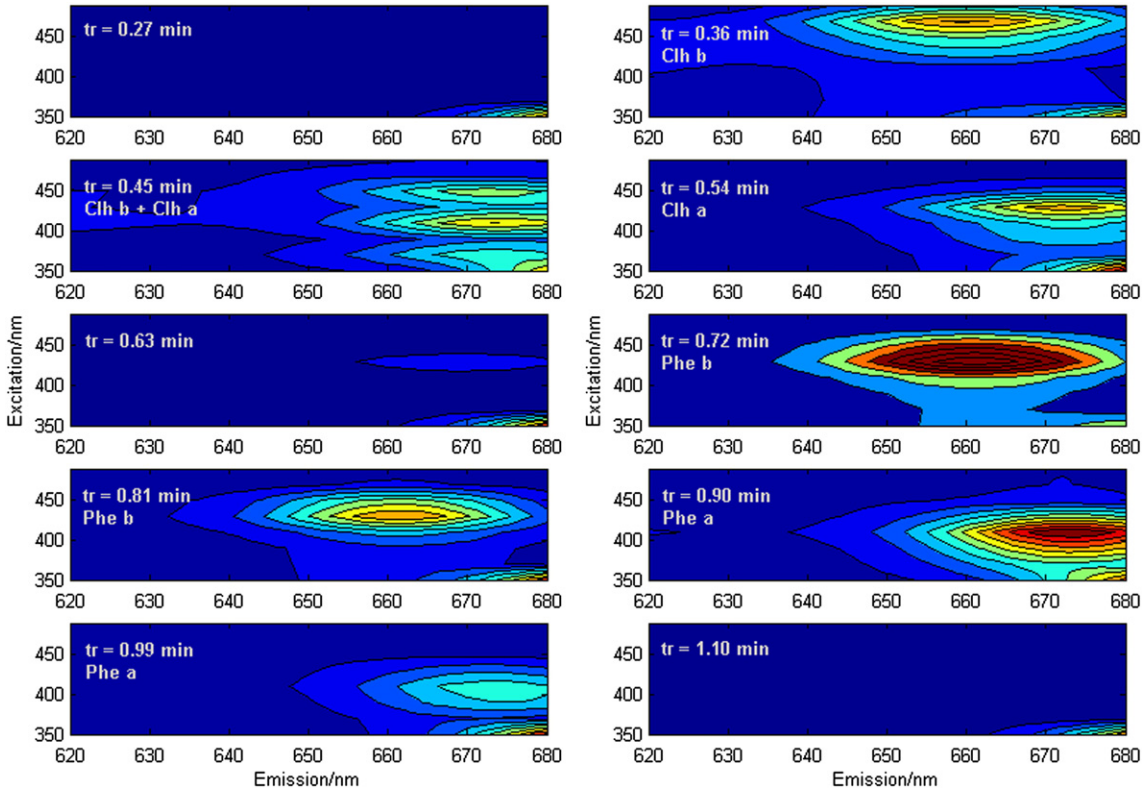

Fig. 5. Contour plots of the EEMs obtained for different retention times (tr) to illustrate the chromatographic evolution of chl *a*, chl *b*, phe *a* and phe *b* of a typical validation sample, containing 1.00 μg mL^{-1} of each compound. Fluorescence intensity has been coded in colors, with deep blue indicating the lowest value and deep red the largest one. The ten contour plots correspond to ten different retention times selected through the chromatogram, from 0.27 min to 1.1 min. (For interpretation of the references to color in this figure, the reader is referred to the web version of this article.)

overlapping and with small irreproducibility in the elution times. On the other hand, these methodologies show the advantage of not requiring the time alignment of the chromatograms, which implies a simplification of the calculations.

Table 3 shows the figures of merit for U-PLS and N-PLS methods. All parameters are seen to be good, indicating that the present methodology may constitute the basis for a simultaneous determination of the four studied analytes. The LODs estimated with both models, according to the literature [54] for the sample of the lowest concentration, were similar to those obtained with dilute solutions of the analytes (Table 3). In this latter case, a solution of each analyte was sequentially diluted with the mobile phase to obtain concentrations in the range from 0.01 to 0.5 μg mL^{-1} (in all cases below the minimum concentration of the calibration set). The detection limit was estimated as the smallest concentration that produced a signal leading to a predicted concentration having an error lower than 5%. With both strategies similar LODs were obtained. The most unfavorable LOD corresponds to chl *b*, due to the low fluorescence intensity of this analyte in the optimized conditions.

The inter-day precision was evaluated by injection of a sample during thirty consecutive days. The recovery values are 113 ± 7 for chl *a*, 102 ± 8 for chl *b*, 93 ± 9 for phe *a* and 100 ± 5 for phe *b*. These values indicate a good repeatability of the multivariate calibration method used.

In order to get further insight into the accuracy and precision of the algorithms analyzed, nominal versus found concentration values were compared by application of the EJCR (elliptical joint confidence region) test. Only the ellipses (at 95% confidence level) of U-PLS and N-PLS include the theoretically expected values of slope = 1 and intercept = 0, as expected. The best results were obtained with the U-PLS and N-PLS algorithms, because the ellipses contain the ideal point and have smaller size, indicating greater accuracy. Nevertheless, PARAFAC does not pass the test because it does not contain the ideal point and shows a large and undesirable size. These results confirm the statistical results shown in Table 2.

4.5. Olive oil samples

With the purpose of testing the applicability of the investigated methods, a set of four olive oils from different varieties was analyzed. The level of chlorophyll pigments depends on genetic factors, the stage of fruit ripeness, the extraction process and the storage conditions. Phe *a* is the major component of the chlorophyll pigments, especially in oils stored for a long time, because during the storage period chlorophyll undergoes specific changes, such as chlorophyll pheophytinization reaction initiated during the extraction process, that implies an alteration of the pigment profile. Phe *a* is present in the olive oil samples analyzed, but the levels of chl *a*, chl *b* and phe *b* are lower than the detection limits of the method and, with the object of carrying out a recovery study, the samples were fortified with the four pigments.

The set of four monovarietal olive oil samples were investigated with the aid of U-PLS and N-PLS, both combined with RTL, constituting a third-order multivariate calibration method capable of achieving the second-order advantage. When U-PLS was applied to these olive oil samples, it was necessary to assess the number of unexpected components (N_{unx}) to be employed in the RTL procedure. This can be done by analyzing the residuals s_u as a function of a trial number of unexpected components. A typical result for one of the analyzed samples was as follows: s_u = 1.84, 0.26 and 0.22 for N_{unx} = 0, 1 and 2, respectively. The choice of N_{unx} = 1 can also be confirmed to be reasonable because, using this value, the predicted analyte concentrations did not significantly change

Table 3
Analytical figures of merit for U-PLS and N-PLS methods in validation[a] and olive oil samples.

	Chl *a*		Chl *b*		Phe *a*		Phe *b*	
	U-PLS	N-PLS	U-PLS	N-PLS	U-PLS	N-PLS	U-PLS	N-PLS
Validation samples								
SEN[b]/mL μg^{-1}	240	230	160	120	170	150	340	330
(γ^{-1})[c]/μg mL^{-1}	0.005	0.006	0.006	0.010	0.007	0.008	0.003	0.003
LOD[d]/μg mL^{-1}	0.04	0.05	0.41	0.46	0.06	0.07	0.05	0.04
LOD[e]/μg mL^{-1}	0.05	0.05	0.40	0.40	0.05	0.05	0.05	0.05
Olive oil samples								
SEN[b]/mL μg^{-1}	170	170	120	120	150	150	250	240
(γ^{-1})[c]/μg mL^{-1}	0.002	0.002	0.002	0.007	0.002	0.003	0.001	0.002
LOD[d]/μg mL^{-1}	0.05	0.05	0.38	0.35	0.07	0.07	0.04	0.04

[a] Figures of merit have been estimated from the sample of lowest concentration.
[b] SEN, sensitivity.
[c] γ^{-1}, inverse of analytical sensitivity (represents the minimum concentration difference which can be measured).
[d] LOD, limit of detection estimated according to ref.54.
[e] Experimental LOD (see text).

with respect to the use of higher number of unexpected components. N-PLS provided comparable results to these obtained with U-PLS. Therefore, one additional component was considered to be necessary in the RTL procedures when the olive oil samples were analyzed, suggesting one unexpected component in the olive oil samples.

Predictions using the U-PLS/RTL model are summarized in Table 4. In all cases, the analytical results are satisfactory taking into account the complexity of the olive oil samples and the absence of pretreatment steps. The average recovery values ranged from 85 to 106%. Similar results have been obtained with N-PLS/RTL model, Table 5.

The found phe *a* contents are in agreement with the bibliographic data and corroborate that this is the principal pigment present in olive oil [31,32]. Its contents in the four olive oils analyzed were: 9.8 mg kg^{-1} for *cornicabra* olive oil, 10.8 mg kg^{-1} for *picual* olive oil, 10.9 mg kg^{-1} for *manzanilla cacereña* olive oil and 21.7 mg kg^{-1} for *hojiblanca* olive oil.

The obtained figures of merit applying U-PLS/RTL and N-PLS/RTL with the olive oil samples (Table 3) are also satisfactory, the detection limits are on the order of 0.04–0.07 μg mL^{-1} for chl *a*, phe *a* and phe *b*, and 0.38 μg mL^{-1} for chl *b*. It should be noted that both algorithms are successful in the presence of unexpected interferences and figures of merit obtained are similar to those for validation samples.

On the other hand, the recovery values are better than those found using the fluorometric method previously proposed by our research group [41]. Also, the use of four-way multivariate calibration allows a significant reduction of the number of samples used for the calibration, and the automation of the analysis of the pigments, something difficult to achieve with the previously described spectroscopic method.

5. Conclusion

This is the first time that four-way data were acquired by following the emission–elution time matrices, at different excitation wavelengths. The four way data, elution time–fluorescence excitation–emission, in combination with advanced third-order chemometric modeling methods, allows the successful determination of chlorophyll and pheophytin pigments in olive oil samples. PARAFAC,U-PLS and N-PLS algorithms were used and compared. U-PLS and N-PLS are genuine higher-order latent variable methods which, once combined with the RTL approach, achieve the second-order advantage needed to successfully quantify the analytes

Table 4
Predicted concentrations in the olive oil samples using U-PLS/RTL.

Olive oil	Added[a]	Chl *a*		Chl *b*		Phe *a*		Phe *b*	
		Found[a]	Rec (%)	Found[a]	Rec (%)	Found[a]	Rec (%)	Found[a]	Rec (%)
Cornicabra		ND		ND		0.10		ND	
	0.55	0.51	93	0.67	122	0.59	89	0.55	100
	0.75	0.77	103	0.75	100	0.77	89	0.75	100
	1.10	1.20	109	1.01	92	1.20	100	1.03	94
Picual		ND		ND		0.11		ND	
	0.40	0.32	80	0.49	122	0.43	80	0.41	103
	0.65	0.51	78	0.68	105	0.69	89	0.63	97
	1.00	0.85	85	0.94	94	0.99	88	0.91	91
Manzanilla cacereña		ND		ND		0.11		ND	
	0.45	0.37	82	0.54	120	0.48	82	0.46	102
	0.80	0.77	96	0.84	105	0.74	80	0.88	110
	0.95	0.78	82	1.00	105	0.98	92	0.90	95
Hojiblanca		ND		ND		0.22		ND	
	0.35	0.27	78	0.39	111	0.49	77	0.34	97
	0.70	0.74	106	0.71	101	0.92	100	0.68	97
	0.90	0.80	89	0.80	89	0.93	80	0.75	83
Rec[b] (%) ± SD		92 ± 12		106 ± 11		88 ± 7		97 ± 7	
RMSEP[c]		0.10		0.07		0.08		0.06	
REP[d] (%)		9		7		8		6	

[a] All values are given in μg mL^{-1}.
[b] Rec, average recovery.
[c] RMSEP, root mean square error prediction.
[d] REP, relative error prediction.

Table 5
Predicted concentrations in the olive oil samples using N-PLS/RTL.

Olive oil		Chl *a*		Chl *b*		Phe *a*		Phe *b*	
	Added[a]	Found[a]	Rec (%)	Found[a]	Rec (%)	Found[a]	Rec (%)	Found[a]	Rec (%)
Cornicabra		ND		ND		0.10		ND	
	0.55	0.52	94	0.63	114	0.58	87	0.56	102
	0.75	0.76	101	0.76	101	0.78	91	0.75	100
	1.10	1.19	108	0.99	90	1.14	94	1.03	94
Picual		ND		ND		0.11		ND	
	0.40	0.32	80	0.51	128	0.41	75	0.41	103
	0.65	0.45	70	0.53	82	0.72	94	0.63	97
	1.00	0.80	80	0.90	90	1.01	90	0.92	92
Manzanilla cacereña		ND		ND		0.10		ND	
	0.45	0.36	80	0.52	116	0.49	87	0.46	102
	0.80	0.73	91	0.75	194	0.82	90	0.87	109
	0.95	0.66	70	0.96	101	1.01	96	0.90	95
Hojiblanca		ND		ND		0.22		ND	
	0.35	0.21	60	0.35	100	0.46	68	0.33	94
	0.70	0.73	104	0.72	103	0.91	98	0.69	98
	0.90	0.75	83	0.76	84	0.96	82	0.75	83
Rec[b] (%) ± SD		85 ± 15		100 ± 14		88 ± 9		97 ± 6	
RMSEP[c]		0.14		0.08		0.08		0.06	
REP[d] (%)		14		8		8		6	

[a] All values are given in μg mL^{-1}.
[b] Rec, average recovery.
[c] RMSEP, root mean square error prediction.
[d] REP, relative error prediction.

in complex samples. The more flexible internal structures of U-PLS/RTL and N-PLS/RTL, in comparison with PARAFAC, make the former two more appropriate approaches for processing four-way data, which are not strictly quadrilinear. The method was applied to the determination of chl *a* and *b* and phe *a* and *b* in olive oil samples without previous treatments. On the other hand, the possibility of analyzing the principal pigments in olive oil samples by the direct injection of the samples dissolved in 1-propanol, without pretreatment steps, represents a great simplification in the analysis. The proposed method is highly selective, requires small quantities of sample, is performed in a short time, and the experimental data can be obtained easily and quickly by the use of an automatic injector, and shows satisfactory recoveries.

Acknowledgments

The authors are grateful to the *Ministerio de Economía y Competitividad* of Spain (Project CTQ2011-25388) co-financed by the European FEDER funds, the *Gobierno de Extremadura* and the European FEDER Funds (Consolidation Project of Research Group FQM003), Project GR1003 , the Universidad Nacional de Rosario, and Consejo Nacional de Investigaciones Científicas y Técnicas (Project PIP1950), for financially supporting this work. The authors thank Dr. A. C. Olivieri for a very stimulating discussion.

References

[1] G.M. Escandar, N.M. Faber, H.C. Goicoechea, A. Muñoz de la Peña, A.C. Olivieri, R.J. Poppi, Second and third-order multivariate calibration: data, algorithms and applications, Trends in Analytical Chemistry 26 (2007) 752–765.
[2] A.C. Olivieri, G.M. Escandar, A. Muñoz de la Peña, Second-order and higher-order multivariate calibration methods applied to non-multilinear data using different algorithms, Trends in Analytical Chemistry 30 (2011) 607–617.
[3] M. Daszykowsky, B.T. Walczak, Use and abuse of chemometrics in chromatography, Trends in Analytical Chemistry 25 (2006) 1081–1096.
[4] A. de Juan, R. Tauler, Chemometrics applied to unravel multicomponent processes and mixtures. Revisiting latest trends in multivariate resolution, Analytica Chimica Acta 500 (2003) 195–210.
[5] C.J. Appellof, E.R. Davidson, Strategies for analyzing data from video fluorometric monitoring of liquid chromatographic effluents, Analytical Chemistry 53 (1981) 2053–2056.
[6] J.L. Beltran, J. Guiteras, R. Ferrer, Three-way multivariate calibration procedures applied to high-performance liquid chromatography coupled with fast-scanning fluorescence spectrometry detection. Determination of polycyclic aromatic hydrocarbons in water samples, Analytical Chemistry 70 (1998) 1949–1955.
[7] R. Ferrer, J. Guiteras, J.L. Beltran, Development of fast-scanning fluorescence spectra as a detection system for high-performance liquid chromatography. Determination of polycyclic aromatic hydrocarbons in water samples, Journal of Chromatography A 779 (1997) 123–130.
[8] S.A. Bortolato, J.A. Arancibia, G.M. Escandar, Non-trilinear chromatographic time retention–fluorescence emission data coupled to chemometric algorithms for the simultaneous determination of 10 polycyclic aromatic hydrocarbons in the presence of interferences, Analytical Chemistry 81 (2009) 8074–8084.
[9] R.A. Gimeno, J.L. Beltran, R.M. Marce, F. Borrull, Determination of naphthalenesulfonates in water by on-lineion-pairsolid-phase extraction and ion-pair liquid chromatography with fast-scanning fluorescence detection, Journal of Chromatography A 890 (2000) 289–294.
[10] F. Cañada Cañada, J.A. Arancibia, G.M. Escandar, G.A. Ibañez, A. Espinosa Mansilla, A. Muñoz de la Peña, A.C. Olivieri, Second-order multivariate calibration procedures applied to high-performance liquid chromatography coupled to fast-scanning fluorescence detection for the determination of fluoroquinolones, Journal of Chromatography A 1216 (2009) 4868–4876.
[11] A. Mancha de Llanos, M.M. de Zan, M.J. Culzoni, A. Espinosa Mansilla, F. Cañada Cañada, A. Muñoz de la Peña, H.C. Goicoechea, Determination of marker pteridines in urine by HPLC with fluorimetric detection and second-order multivariate calibration using MCR-ALS, Analytical and Bioanalytical Chemistry 399 (2011) 2123–2135.
[12] M.J. Culzoni, A. Mancha de Llanos, M.M. de Zan, A. Espinosa Mansilla, F. Cañada Cañada, A. Muñoz de la Peña, H.C. Goicoechea, Enhanced MCR-ALS modeling of HPLC with fast scan fluorimetric detection second-order data for quantitation of metabolic disorder marker pteridines in urine, Talanta 85 (2011) 2368–2374.
[13] C.M. Andersen, R. Bro, Practical aspects of PARAFAC modelling of fluorescence excitation–emission data, Journal of Chemometrics 17 (2003) 200–215.
[14] A.C. Olivieri, J.A. Arancibia, A. Muñoz de la Peña, I. Durán Merás, A. Espinosa Mansilla, Second-order advantage achieved with four-way fluorescence excitation–emission-kinetic data processed by parallel factor analysis and trilinear least-squares. Determination of methotrexate and leucovorin in human urine, Analytical Chemistry 76 (2004) 5657–5666.
[15] J.A. Arancibia, A.C. Olivieri, D. Bohoyo Gil, A. Espinosa Mansilla, I. Durán Merás, A. Muñoz de la Peña, Trilinear least-squares and unfolded-PLS coupled to residual trilinearization: new chemometric tools for the analysis of four-way instrumental data, Chemometrics and Intelligent Laboratory Systems 80 (2006) 77–86.
[16] A. Muñoz de la Peña, I. Durán Merás, A. Jiménez Girón, H.C. Goicoechea, Evaluation of unfolded-partialleast-squares coupled to residual trilinearization for four-way calibration of folic acid and methotrexate in human serum samples, Talanta 72 (2007) 1261–1267.
[17] A. Jiménez Girón, I. Durán Merás, A. Espinosa Mansilla, A. Muñoz de la Peña, F. Cañada Cañada, A.C. Olivieri, On line photochemically induced excitation–emission-kinetic four-way data: analytical application for the determination of folic acid and its two main metabolites in serum by U-PLS and N-PLS/residual trilinearization (RTL) calibration, Analytica Chimica Acta 622 (2008) 94–103.
[18] P.C. Damiani, I. Durán Merás, A.G. García Reiriz, A. Jiménez Girón, A. Muñoz de la Peña, A.C. Olivieri, Multiway partial least-squares coupled to residual trilinearization: a genuine multidimensional tool for the study of third-order data. Simultaneous analysis of procaine and its metabolite p-aminobenzoic acid in equine serum, Analytical Chemistry 79 (2007) 6949–6958.

[19] J. Jaumot, V. Marchán, R. Gargallo, A. Grandas, R. Tauler, Multivariate curve resolution applied to the analysis and resolution of two-dimensional [^{1}H,^{15}N] NMR reaction spectra, Analytical Chemistry 76 (2004) 7094–7101.
[20] Y. Tan, J.H. Jiang, H.L. Wu, H. Cui, R.Q. Yu, Resolution of kinetic system of simultaneous degradations of chlorophyll *a* and *b* by PARAFAC, Analytica Chimica Acta 412 (2000) 195–202.
[21] R.P.H. Nikolajsen, K.S. Booksh, A.M. Hansen, R. Bro, Quantifying catecholamines using multi-way kinetic modeling, Analytica Chimica Acta 475 (2003) 137–150.
[22] A. Muñoz de la Peña, I. Durán Merás, A. Jiménez Girón, Four-way calibration applied to the simultaneous determination of folic acid and methotrexate in urine samples, Analytical and Bioanalytical Chemistry 385 (2006) 1289–1297.
[23] A.L. Xia, H.L. Wu, S.F. Li, S.H. Zhu, L.Q. Hu, R.Q. Yu, Alternating penalty quadrilinear decomposition algorithm for an analysis of four-way data arrays, Journal of Chemometrics 21 (2007) 133–144.
[24] S.H. Zhu, H.L. Wu, A.L. Xia, J.F. Nie, Y.C. Bian, C.B. Cai, R.Q. Yu, Excitation–emission-kinetic fluorescence coupled with third-order calibration for quantifying carbaryl and investigating the hydrolysis in effluent water, Talanta 77 (2009) 1640–1646.
[25] R.M. Maggio, P.C. Damiani, A.C. Olivieri, Four-way kinetic-excitation–emission fluorescence data processed by multi-way algorithms. Determination of carbaryl and 1-naphthol in water samples in the presence of fluorescent interferents, Analytica Chimica Acta 677 (2010) 97–107.
[26] A.G. García Reiriz, P.C. Damiani, A.C. Olivieri, F. Cañada Cañada, A. Muñoz de la Peña, Nonlinear four-waykinetic-excitation–emission fluorescence data processed by a variant of parallel factor analysis and by a neural network model achieving the second-order advantage: malonaldehyde determination in olive oil sample, Analytical Chemistry 80 (2008) 7248–7256.
[27] Y.C. Kim, J.A. Jordan, M.L. Nahorniak, K.S. Booksh, Photocatalytic degradation–excitation–emission matrix fluorescence for increasing the selectivity of polycyclic aromatic hydrocarbon analyses, Analytical Chemistry 77 (2005) 7679–7686.
[28] M.L. Nahorniak, G.A. Cooper, Y.C. Kim, K.S. Booksh, Three- and four-way parallel factor (PARAFAC) analysis of photochemically induced excitation–emission kinetic fluorescence spectra, Analyst 130 (2000) 585–593.
[29] A.E. Sinha, B.J. Prazen, R.E. Synovec, Trends in chemometric analysis of comprehensive two-dimensional separations, Analytical and Bioanalytical Chemistry 378 (2004) 1948–1951.
[30] M.I. Mínguez Mosquera, B. Gandul Rojas, M.L. Gallardo Guerrero, Rapid method of quantification of chlorophylls and carotenoids in virgin olive oil by high-performance liquid chromatography, Journal of Agricultural and Food Chemistry 40 (1992) 60–63.
[31] E. Psomiadou, M. Tsimidou, Simultaneous HPLC determination of tocopherols, carotenoids, and chlorophylls for monitoring their effect on virgin olive oil oxidation, Journal of Agricultural and Food Chemistry 46 (1998) 5132–5138.
[32] M. Roca, B. Gandul Rojas, L. Gallardo Guerrero, M.I. Mínguez Mosquera, Pigment parameters determining Spanish virgin olive oil authenticity: stability during storage, Journal of the American Oil Chemists' Society 80 (2003) 1237–1240.
[33] A. Serani, D. Piacenti, Analytical system for identification of deodorized oils in virgin olive oil. Note 1: analysis of chlorophyll pigments in virgin olive oils, Rivista Italiana Delle Sostanze Grasse 78 (2001) 459–463.
[34] R. Mateos, J.A. García Mesa, Rapid and quantitative extraction method for the determination of chlorophylls and carotenoids in olive oil by high performance liquid chromatography, Analytical Biochemistry 385 (2006) 1247–1254.
[35] Q. Su, K.G. Rowley, C. Itsiopoulos, K. O'Dea, Identification and quantitation of major carotenoids in selected components of the Mediterranean diet: green leafy vegetables, figs and olive oil, European Journal of Clinical Nutrition 56 (2002) 1149–1154.
[36] P. Luaces, A.G. Pérez, J.M. García, C. Sanz, Effects of heat-treatments of olive fruit on pigment composition of virgin olive oil, Food Chemistry 90 (2005) 169–174.
[37] A. Cichelli, G.P. Pertesana, High-performance liquid chromatographic analysis of chlorophylls, pheophytins and carotenoids in virgin olive oils: chemometric approach to variety classification, Journal of Chromatography. A 1046 (2004) 141–146.
[38] L. Moberg, G. Robertsson, B. Karlberg, Spectrofluorimetric determination of chlorophylls and pheopigments using parallel factor analysis, Talanta 54 (2001) 161–170.
[39] L. Moberg, B. Karlberg, Validation of a multivariate calibration method for the determination of chlorophyll a, b and c and their corresponding pheopigments, Analytica Chimica Acta 450 (2001) 143–153.
[40] L. Moberg, B. Karlberg, S. Blomqvist, U. Larsson, Comparison between a new application of multivariate regression and current spectroscopy methods for the determination of chlorophylls and their corresponding pheopigments, Analytica Chimica Acta 411 (2000) 137–143.
[41] T. Galeano Díaz, I. Durán Merás, C. Arturo Correa, B. Roldan, M.I. Rodríguez Cáceres, Simultaneous fluorometric determination of chlorophylls a and b and pheophytins a and b in olive oil by partial least-squares calibration, Journal of Agricultural and Food Chemistry 51 (2003) 6934–6940.
[42] MATLAB, version 7, The MathWorks Inc., Natick, Massachusetts2010.
[43] A.C. Olivieri, H.L. Wu, R.Q. Yu, MVC3: a MATLAB graphical interface toolbox for third-order multivariate calibration, Chemometrics and Intelligent Laboratory Systems 116 (2012) 9–16.
[44] S. Leurgans, R.T. Ross, Multilinear models: applications in spectroscopy, Statistical Science 7 (1992) 289–319.
[45] R. Bro, PARAFAC. Tutorial and applications, Chemometrics and Intelligent Laboratory Systems 38 (1997) 149–171.
[46] P. Paatero, A weighted non-negative least squares algorithm for three-way "PARAFAC" factor analysis, Chemometrics and Intelligent Laboratory Systems 38 (1997) 223–242.
[47] http://www.models.kvl.dk/source/.
[48] R. Bro, Multi-way Analysis in the Food Industry. Doctoral Thesis University of Amsterdam, Netherlands1998.
[49] R. Bro, H.A.L. Kiers, A new efficient method for determining the number of components in PARAFAC models, Journal of Chemometrics 17 (2003) 274–286.
[50] S. Wold, P. Geladi, K. Esbensen, J. Øhman, Multi-way principal components- and PLA-analysis, Journal of Chemometrics 1 (1987) 41–56.
[51] D.M. Haaland, E.V. Thomas, Partial least-squares methods for spectral analyses. 1. Relation to other quantitative calibration methods and the extraction of qualitative information, Analytical Chemistry 60 (1988) 1193–1202.
[52] G.R. Seely, R.G. Jensen, Effect of solvent on the spectrum of chlorophyll, Spectrochimica Acta 21 (1965) 1835–1845.
[53] G. Weber, F.W.J. Teale, Determination of the absolute quantum yield of fluorescent solutions, Transactions of the Faraday Society 53 (1957) 646–655.
[54] S.A. Bortolato, J.A. Arancibia, G.M. Escandar, Chemometrics-assisted excitation–emission fluorescence spectroscopy on nylon membranes. Simultaneous determination of benzo[a]pyrene and dibenz[a, h]anthracene at parts-per-trillion levels in the presence of the remaining EPA PAH priority pollutants as interferences, Analytical Chemistry 80 (2008) 8276–8286.